Mapping the Spatial Distribution of H_2 in Nearby Galaxies with the *Spitzer* Infrared Spectrograph

Gregory Brunner[1], Reginald Dufour[1], Kartik Sheth[2], Lee Armus[2], Stuart Vogel[3], Mark Wolfire[3], Eva Schinnerer[4]

ABSTRACT

In order to understand the connection between the warm (T = 100 – 1000 K) molecular gas traced by the pure rotational mid-infrared H_2 lines and the cold (T $<$ 100 K) molecular gas traced by CO ($J = 1 - 0$), we have undertaken a program to map the spatial distribution of pure rotational H_2 line emission in nearby galaxies with the *Spitzer Space Telescope* Infrared Spectrograph (IRS). Using our own Spitzer IRS spectral mapping mode observations of M51 and archival Spitzer IRS spectral mapping observations acquired as part of the Spitzer Infrared Nearby Galaxies Survey (SINGS) and other observing programs, we have mapped the spatial distribution of warm molecular gas traced by the H_2 S(0) – H_2 S(3) pure rotational lines in nearby galaxies. Here, we present maps of the H_2 S(0) – H_2 S(3) line emission for M51, NGC 628, NGC 3351, and NGC 3521 and compare the H_2 emission distributions to the cold molecular gas distributions traced by CO emission observed as part of the Berkeley-Illinois-Maryland Association Survey of Nearby Galaxies (BIMA SONG). We show that the H_2 emission distributions are generally spatially coincident with the CO emission; although, some offsets between the H_2 and CO are noted.

Subject headings: galaxies: ISM — infrared: galaxies — H_2

[1]Department of Physics and Astronomy, Rice University, Houston, TX 77005

[2]Spitzer Science Center, Caltech, Pasadena, CA 91125

[3]Department of Astronomy, University of Maryland, College Park, MD 20741

[4]Max-Planck-Institut für Astronomie, Königstuhl 17, 69117 Heidelberg, Germany

1. Introduction

The pure rotational mid-infrared H_2 emission lines provide a powerful probe of the physical conditions of the warm molecular interstellar medium (ISM). Surveys of pure rotational H_2 line emission in nearby galaxies with the Infrared Space Observatory (ISO) and Spitzer Space Telescope (*Spitzer*) have found warm H_2 temperatures ranging from 100 K – 300 K and warm-to-cold molecular gas mass fractions that range from ~ 0.01 – 0.30 (Rigopoulou et al. 2002, Roussel et al. 2007, Brunner et al. 2008). While these surveys of warm H_2 in nearby galaxies have led to a better understanding of the warm ISM, many questions remain unanswered. How does H_2 emission vary on sub-kiloparsec scales within galaxies? Where is the H_2 emission being excited (i.e. in photodissociation regions (PDRs), around an active galactic nucleus (AGN), or by shocks)? How does the warm-to-cold H_2 mass ratio vary as a function of position across a galaxy?

In order to address these questions, we have undertaken an archival program (PID #40773; PI: G. Brunner) to map the spatial distribution of H_2 emission in nearby galaxies observed with the *Spitzer* Infrared Spectrograph (IRS) in spectral mapping mode and the Berkeley-Illinois-Maryland Association Survey of Nearby Galaxies (BIMA SONG) (Regan et al. 2001, Helfer et al. 2003). In this paper, we discuss results from our program for 4 galaxies: NGC 628, NGC 3351, NGC 3521, and M51. For each galaxy, we present maps the of spatial distribution of H_2 S(0) – H_2 S(3) emission and compare the H_2 S(1) emission to the CO ($J = 1 - 0$) data from BIMA SONG.

2. Observations and Data Reduction

In order to study the spatial distribution of H_2 in nearby galaxies, we used *Spitzer* IRS low resolution spectral mapping mode observations that have been acquired through the Spitzer Infrared Nearby Galaxies Survey (SINGS; Kennicutt et al. 2003) and other individual IRS spectral mapping programs of galaxies such as M51 (PID: 20138; PI: K. Sheth). The IRS spectral mapping footprints of M51, NGC 628, NGC 3351, and NGC 3521 are shown in Figure 1. For each galaxy, data cubes of the IRS Short-Low (SL) and Long-Low (LL) spectra were constructed using CUBISM (Smith et al. 2007a). For galaxies observed by SINGS, we used the publicly available SL and LL data cubes[1].

[1]SINGS data cubes can be downloaded at http://irsa.ipac.caltech.edu/data/SPITZER/SINGS/galaxies/. For additional information about SINGS data products, the reader is referenced to the SINGS Fifth Data Delivery found at http://ssc.spitzer.caltech.edu/legacy/singshistory.html.

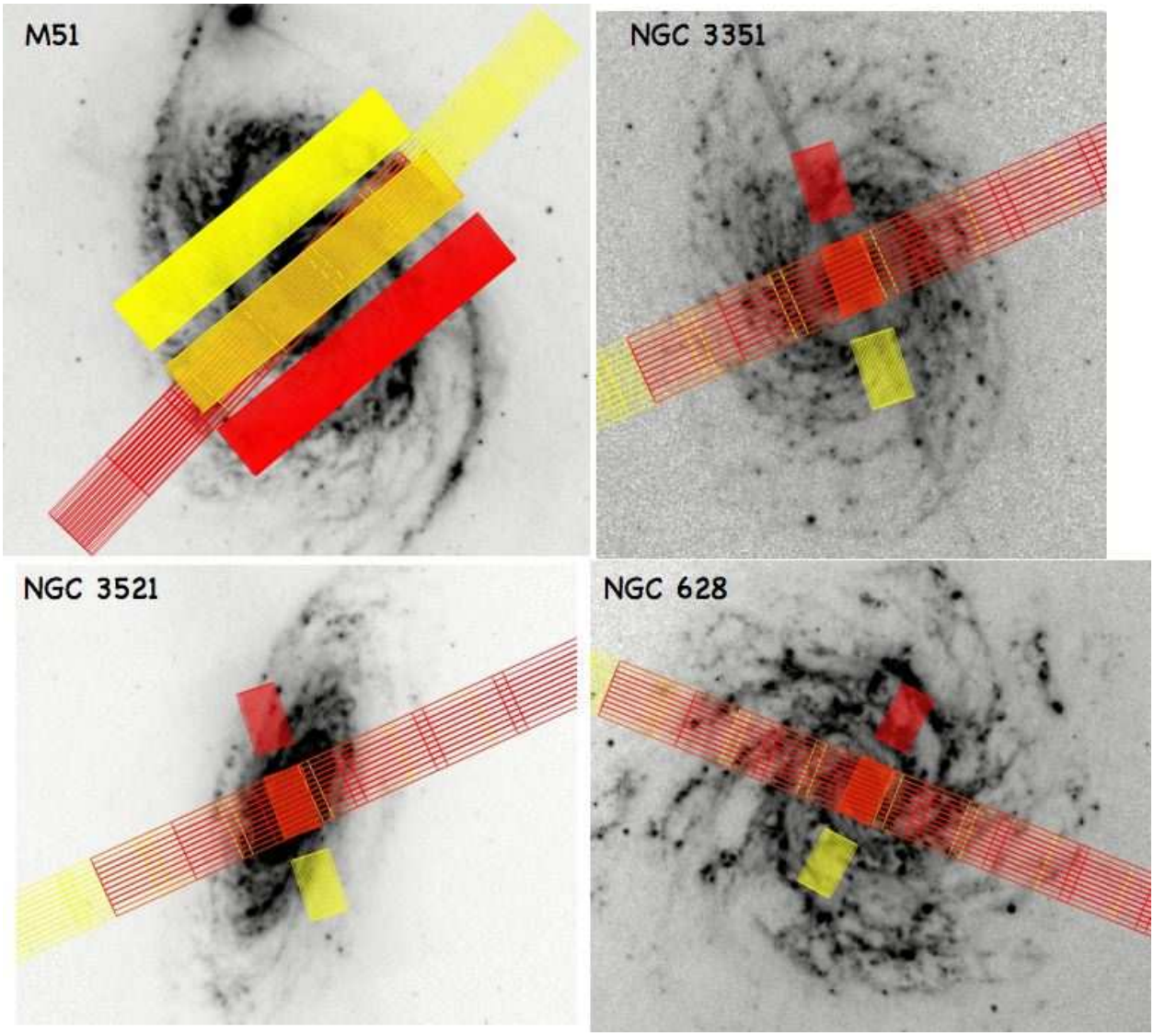

Fig. 1.— The *Spitzer* IRS SL and LL spectral mapping footprints plotted over the IRAC 8 μm image for the 4 galaxies presented in this paper. The three parallel rectangles mark the SL (5 – 14.5 μm) observations with the yellow rectangles denoting the SL2 (5 – 7.5 μm) coverage and the red rectangles denoting the SL1 (7.5 – 14.5 μm) coverage. The single, long central strip marks the LL (14 – 38 μm) observations with the yellow representing the LL2 (14 – 21 μm) coverage and the red representing the LL1 (20.5 – 38 μm) coverage.

We created continuum-subtracted, extinction-corrected maps of emission from the pure rotational H_2 S(0) 28.22 μm, H_2 S(1) 17.04 μm, H_2 S(2) 12.28 μm, and H_2 S(3) 9.66 μm lines for each galaxy with a our own PAHFIT-based (Smith et al. 2007b) *Spitzer* IRS spectral cube decomposition code. This is the same code used to produce the H_2 emission distributions of M51 presented in Brunner et al. (2008).

3. Results

3.1. H_2 Emission Distributions

In Figure 2, we present the H_2 S(0) – H_2 S(3) emission distributions for M51, NGC 628, NGC 3351, and NGC 3521. In Figure 3, we compare the H_2 S(1) emission distribution to CO emission for each galaxy. A discussion of the emission distributions and comparison to the CO maps for the individual galaxies is given below.

3.1.1. M51

In M51, the warm H_2 temperature peaks in the nuclear region at 192 K and decreases to 150 – 165 K in the spiral arms. The column density in the nuclear region is 2.5 $M_\odot/\,\mathrm{pc}^{-2}$ and increases to a maximum of 11 $M_\odot/\,\mathrm{pc}^{-2}$ in the northwest inner spiral arm (Brunner et al. 2008). The warm H_2 is generally co-spatial with the CO in the spiral arms suggesting that the warm H_2 is associated with the surface layers of molecular clouds.

3.1.2. NGC 628

Maps of the H_2 S(0) and H_2 S(1) lines show that the locations of the brightest H_2 emission in NGC 628 are different for these two lines. The H_2 S(0) emission peaks in the northeast spiral arm whereas the H_2 S(1) emission is brightest in the spiral arm to the south of the nucleus. These differences in peak emission suggest variations in H_2 temperature, ortho-to-para ratio (OPR), and density. Faint, clumpy emission from the H_2 S(2) and H_2 S(3) lines is seen outside of the nucleus of the galaxy. In NGC 628, the brightest CO emission is also observed outside of the nuclear region (Regan et al. 2001). The H_2 S(1) emission is generally co-spatial with the CO emission; although, some differences in the emission distributions are noted, such as in the spiral arm to the south of the nucleus where the H_2 S(1) emission is brightest.

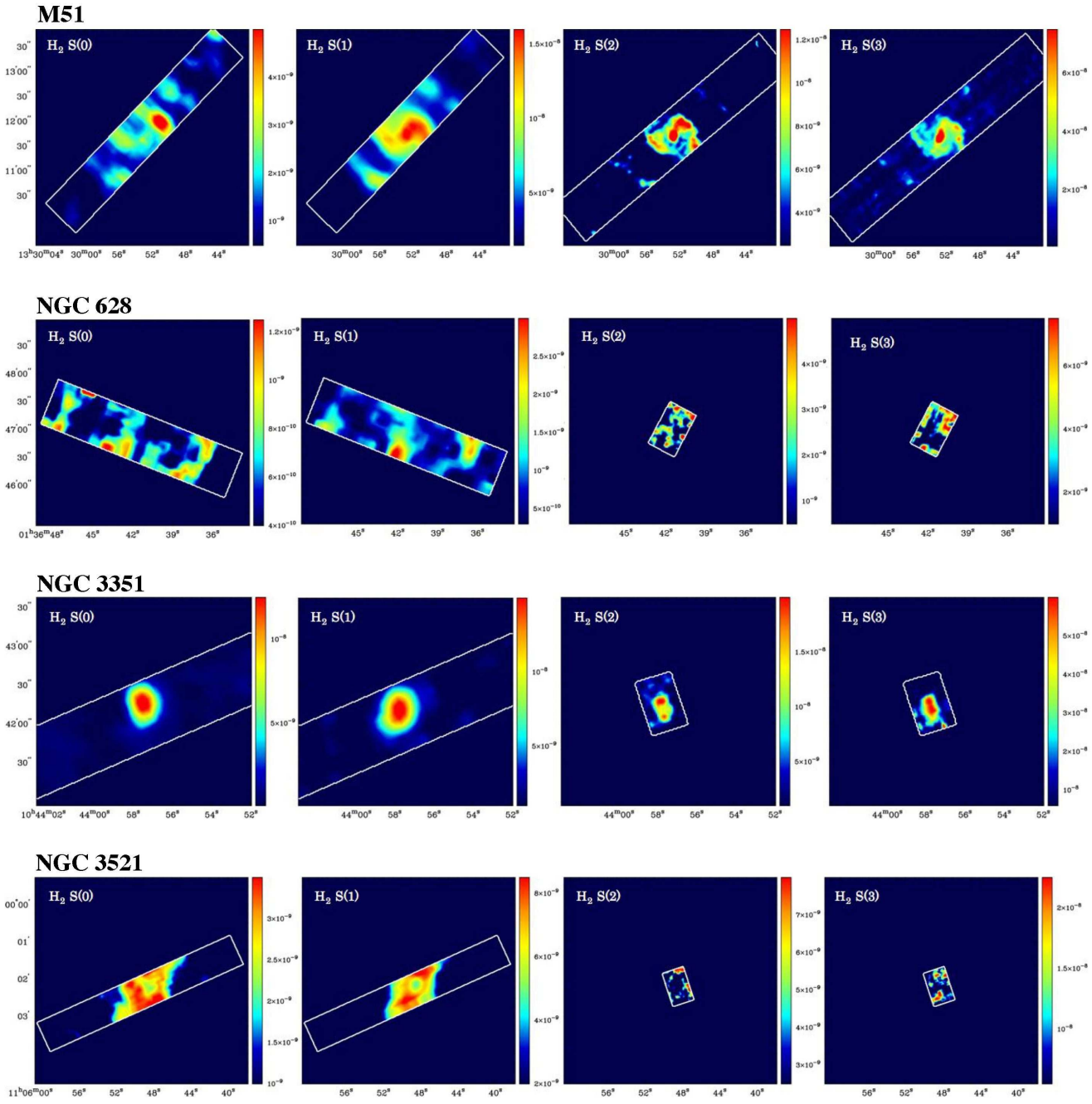

Fig. 2.— Maps of the H_2 S(0) – H_2 S(3) lines across M51, NGC 628, NGC 3351, and NGC 3521 (in order from top to bottom). The color bars are in units of W m^{-2} sr^{-1}. For each galaxy, note the spatial variations in the emission distributions for each H_2 line.

3.1.3. NGC 3351

Slight offset in the peak of the emission from the H_2 S(0) and H_2 S(1) lines is evident in the nuclear region. Emission from the H_2 S(2) and H_2 S(3) lines shows "twin peaks," similar to the emission distribution of CO in the nuclear region of NGC 3351 observed by Kenney et al. (1992). The "twin peaks" in emission from the H_2 S(3) line appear closer to each other than the peaks seen in the H_2 S(2) map. While the H_2 S(0) and H_2 S(1) lines do not show the "twin peak" morphology that the H_2 S(2) and H_2 S(3) lines show, this difference is probably due to the difference in resolution between the SL and LL modules.

3.1.4. NGC 3521

The H_2 S(0) and H_2 S(1) lines show similar overall emission distributions with emission being brighter in the circumnuclear region than in the nucleus. Differences in the locations of emission peaks from the H_2 S(0) and H_2 S(1) lines are evident. The H_2 S(2) and H_2 S(3) lines show much smaller clumpy emission outside of the nucleus of the galaxy. All H_2 lines show a lack of emission from the central region of the galaxy; however, the H_2 S(2) and H_2 S(3) lines show very different emission distributions compared to the H_2 S(0) and H_2 S(1) lines.

4. Summary

For each galaxy, the overall emission distributions are similar for each H_2 line, but details in the morphologies are different, suggesting variations in warm H_2 temperature, OPR, and column density across the disks. Further investigation is needed in order to understand how these differences translate into quantitative variations in H_2 temperature, OPR, and column density for each galaxy. We also compare the H_2 S(1) emission distributions to the CO emission distributions from BIMA SONG and we see that the H_2 is generally co-spatial with the CO emission, though some offsets in peak emission can be seen, for example, in the spiral arm to the south of the nuclear region of NGC 628.

This work is based on observations and archival data obtained with the *Spitzer Space Telescope*, which is operated by the Jet Propulsion Laboratory, California Institute of Technology under a contract with NASA. Support for this work was provided by an award issued by JPL/Caltech.

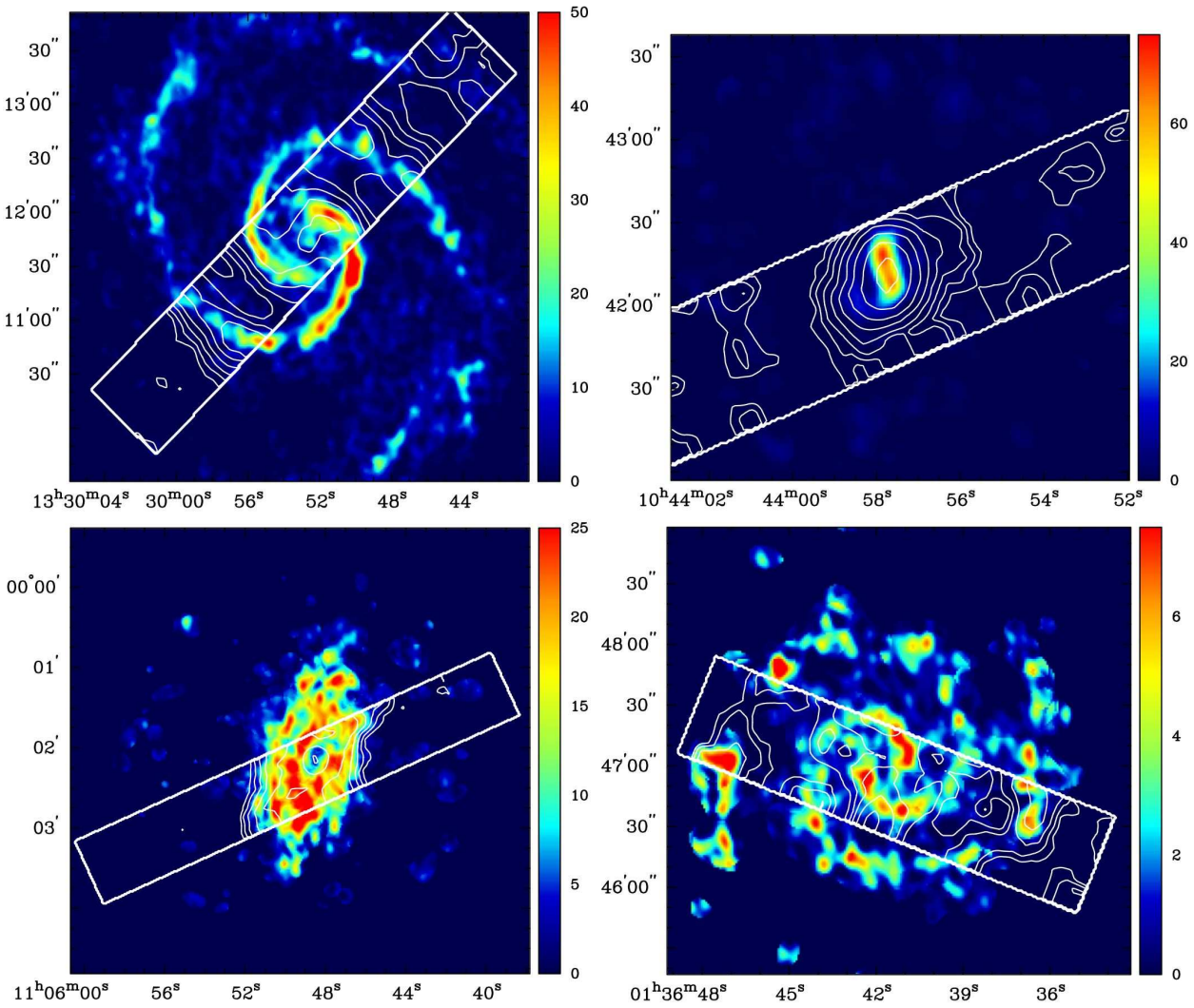

Fig. 3.— Comparison of the CO emission (in color) to the H_2 S(1) (in contours) emission for M51 (*top left*), NGC 3351 (*top right*), NGC 3521 (*bottom left*), and NGC 628 (*bottom right*). The color bar is in units of Jy km s^{-1}. For M51, contours are on a logarithmic scale from 1.5×10^{-9} to 1.5×10^{-8} W m^{-2} sr^{-1}. For NGC 3351, contours are on a logarithmic scale from 1.0×10^{-9} to 1.5×10^{-8} W m^{-2} sr^{-1}. For NGC 3521, contours are on a logarithmic scale from 2.0×10^{-9} to 8.5×10^{-9} W m^{-2} sr^{-1}. For NGC 628, contours are on a logarithmic scale from 6.0×10^{-10} to 3.0×10^{-9} W m^{-2} sr^{-1}.

REFERENCES

Brunner, G. et al., 2008, ApJ, 675, 316

Helfer, T. et al., 2003, ApJS, 145, 259

Kenney, J.D.P. et al., 1992, ApJ, 395, 79

Kennicutt, R.C. et al., 2003, PASP, 115, 928

Regan, M. et al., 2001, ApJ, 561, 218

Rigoupoulou, D. et al., 2002, A&A, 389, 374

Roussel, H. et al., 2007, ApJ, 669, 959

Smith, J.D. et al., 2007a, PASP, 119, 1133

Smith, J.D. et al., 2007b, ApJ, 656, 770